Evidence for nascent equilibrium nuclei as progenitors of anomalous transformation kinetics in a Pu-Ga alloy

J. R. Jeffries, K. J. M. Blobaum, M. A. Wall, and A. J. Schwartz
Lawrence Livermore National Laboratory, Livermore, California 94550, USA
(Received 9 July 2009; revised manuscript received 18 August 2009; published 17 September 2009)

By alloying Pu with Ga, the face-centered-cubic δ phase can be retained down to room temperature in a metstable configuration, which ultimately yields to chemical driving forces by undergoing the $\delta \rightarrow \alpha'$ isothermal martensitic transformation below $M_s \approx -100$ °C. This transformation is found to exhibit anomalous transformation kinetics, the nature of which has remained elusive for over 30 years. Recently, a "conditioning" treatment—an isothermal hold above M_s—has been shown to dramatically affect the amount of α' phase formed during the transformation. Herein, we report evidence that the conditioning treatment induces the lower C of the double-C curve and we furthermore implicate the classical nucleation of equilibrium phases as the underlying mechanism of the conditioning effect in Pu-Ga alloys. This mechanism should not be rigorously exclusive to plutonium alloys as it arises from the proximity of energies between the retained metastable phase and the low-energy equilibrium phases.

DOI: 10.1103/PhysRevB.80.094107 PACS number(s): 81.30.Bx, 81.30.Kf, 81.40.Ef

I. INTRODUCTION

Alloying plutonium with gallium yields a complex equilibrium Pu-Ga phase diagram reflective of the multiple, nearly degenerate phases of the pure element.[1–5] The rich phase diagram of Pu-Ga is no doubt dominated by the effects of *f*-electron correlation[6–11] and the differences between the properties of ground state α-Pu and δ-Pu serve as prime examples of how these strong correlations can induce dramatically different macroscopic properties including crystal symmetry, ductility, Sommerfeld coefficient, magnetic susceptibility, thermal expansion, etc.[3,12,13] As yet, a complete picture regarding the fundamental factors that ultimately drive plutonium between the α and δ phases is lacking. In fact, the sources of entropy responsible for stabilizing δ-Pu in favor of α-Pu are currently unaccounted for.[14] The α and δ phases of plutonium as well as transitions between them are key components to our understanding of the role that *f*-electron correlation plays in engendering the phase stability and physical properties of actinide metals, alloys, and compounds.

The lean gallium (Ga content $\leq$10 at. %) portion of the equilibrium Pu-Ga phase diagram displays no fewer than 13 solid-state phase fields as shown in Fig. 1(a). Of these phase fields, only three are single phase where Ga exhibits appreciable solubility: the face-centered-cubic δ phase, the body-centered-tetragonal δ' phase, and the body-centered-cubic ϵ phase. The balance of the phase fields exist as mixed phase regions consisting of combinations of Ga-miscible, Ga-immiscible, and ordered phases.[15,16] While increased Ga content tends to stabilize the δ phase toward lower temperatures, it is the slow Ga diffusion within the δ phase that likely permits it to be retained in a metastable state down to room temperature or below [Fig. 1(a)], well within several of the mixed phase fields.[3–5,17] In addition to the limited Ga diffusion in the δ phase, self-irradiation effects from the alpha decay of ^{239}Pu prohibit true equilibrium by altering chemical composition and lattice periodicity through the accumulation of daughter products, helium bubbles, and defects.[18–21]

The metastable δ phase of the Pu-Ga system can be unstable toward transformation to the metastable α' martensite, which occurs at subambient temperatures for Ga concentrations between about 0.6 and 2.5 at. %.[16,22,23] The α' product phase forms with the same structure as α-Pu but the diffusionless character of the transformation traps Ga solute and expands the lattice.[22,23] This $\delta \rightarrow \alpha'$ transformation is incomplete, resulting in only about 25% α' product by volume due to the strains associated with the large unit-cell volume discrepancy between the parent and product phases. For the case of a Pu-1.9 at. % Ga alloy, the $\delta \rightarrow \alpha'$ transformation yields the α' martensitic phase isothermally (i.e., a temperature-dependent incubation time is required) with peculiar double-C kinetics when plotted on a time-temperature-transformation (TTT) diagram [see Fig. 1(b)], on which *two* temperatures define minimum times for the initiation of transformation.[24,25] While double-C kinetics have been observed and explained in other systems,[26,27] the nature of the double C in Pu-Ga has defied explanation for over three decades and remains a perplexing component of plutonium science. Understanding the kinetics and mechanisms of the $\delta \rightarrow \alpha'$ martensite in Pu-Ga has profound implications on our appreciation of phase stability in actinides and of martensitic transformations in general.

Recent research has shown that a "conditioning" treatment—which entails an isothermal hold of order hours below a 375 °C anneal but above M_s—enhances the amount of transformation occurring at low temperature.[28] This conditioning effect seems contrary to conventional metallurgical precepts, where subanneal temperatures should represent vanishingly small perturbations to the system. While these results certainly engender questions surrounding the essential characteristics of conditioning, they also reveal an opportunity to probe the double C in Pu-Ga alloys by studying the nature of this conditioning treatment and its role in the $\delta \rightarrow \alpha'$ transformation. Here we report results of the impact of conditioning on the $\delta \rightarrow \alpha'$ transformation as well as a detailed study designed to illuminate the nature of conditioning. We invoke a nucleation mechanism to explain the ob-

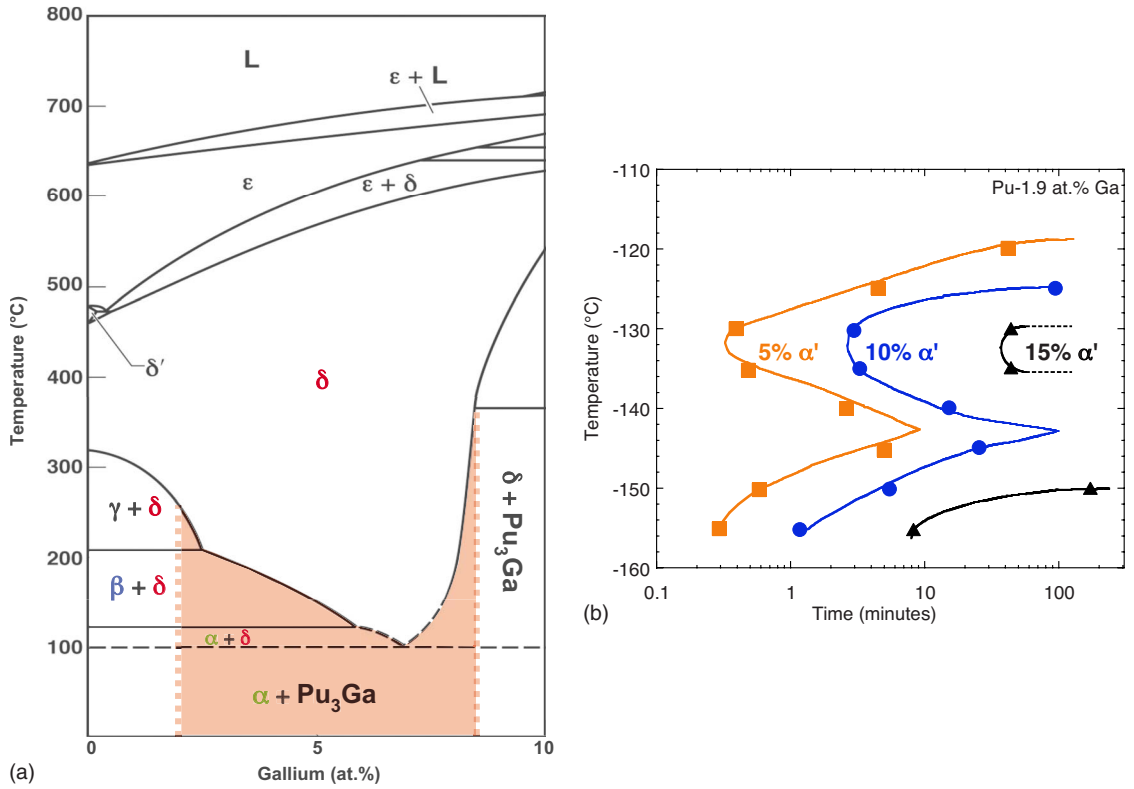

FIG. 1. (Color online) (a) The low-Ga portion of the phase diagram of the Pu-Ga system shows the multiple stable equilibrium phases.[23] The red, shaded area bounded by vertical dashed lines represents the region of the phase diagram where the metastable δ phase likely persists due to slow Ga diffusion. (b) The TTT diagram of a Pu-1.9 at. % Ga alloy shows anomalous double-C behavior where the $\delta \rightarrow \alpha'$ transformation occurs in a minimum amount of time at two distinct temperatures.[24]

served temperature dependencies and transformation-promoting effects of conditioning.

II. EXPERIMENTAL DETAILS

The optical metallography experiments have been described previously[29] and a sample with the same chemical composition from the same casting was used in the differential scanning calorimetry (DSC) experiments. The Fe content of this sample, 0.1755 at. % (410 ppm by weight), is not atypical for Pu specimens. The Fe impurities predominantly reside on grain boundaries as Pu_6Fe inclusions, which are unlikely to affect the bulk behavior of phase transformations in Pu-Ga.[30] Polycrystalline samples of Pu-1.9 at. % Ga were machined into ~3 mm diameter disks with a mass of 177 mg and loaded into Au-plated stainless steel pans. To ensure a single-phase specimen with a homogeneous Ga distribution, the sample was annealed for 534 h at 460 °C.

Differential scanning calorimetry data was acquired in a power compensating Perkin-Elmer Pyris Diamond differential scanning calorimeter previously calibrated with adamantane, indium, and zinc. Preceding each individual experiment, the sample was annealed at 375 °C in the DSC to revert any previous α' product to the δ phase and to eliminate defects and strains accumulated from prior martensitic transformation.[31] Continuous cooling DSC traces were obtained at 20 °C/min. A smooth baseline was subtracted from the data to yield the portion of the DSC trace associated with the transformation of the sample.

III. EXPERIMENTAL SIGNATURES OF CONDITIONING

The dramatic effects of conditioning on the $\delta \rightarrow \alpha'$ transformation are highlighted in the optical metallography images of Figs. 2(a) and 2(b). The upper-right triangular portion of each subfigure represents a sample that has been conditioned while the lower-left triangular portion represents an unconditioned sample. Embedded in the δ matrix (background of each image) are acicular features corresponding to the α' product phase. Figure 2(a) corresponds to a sample that was quenched to −120 °C and held for 4 h (upper C of the TTT diagram) while Fig. 2(b) represents a sample that was quenched to −155 °C and held for 4 h (lower C of the TTT diagram). In the upper C, conditioning enhances the amount of transformation that occurs upon cooling, as indicated by the increase in the size and number of α' particles. However, the overall morphology of the transformation in the upper C is substantially equivalent irrespective of conditioning, suggesting that conditioning only affects the amount of transformation and not the martensitic mechanism. The conditioning dependence in the lower C is markedly different from that of the upper C: without conditioning, no transformation is visible above the resolution limit ($\approx 3\ \mu m^2$) of our optical metallography; with conditioning, a large amount of transformation is evident. This observation suggests that con-

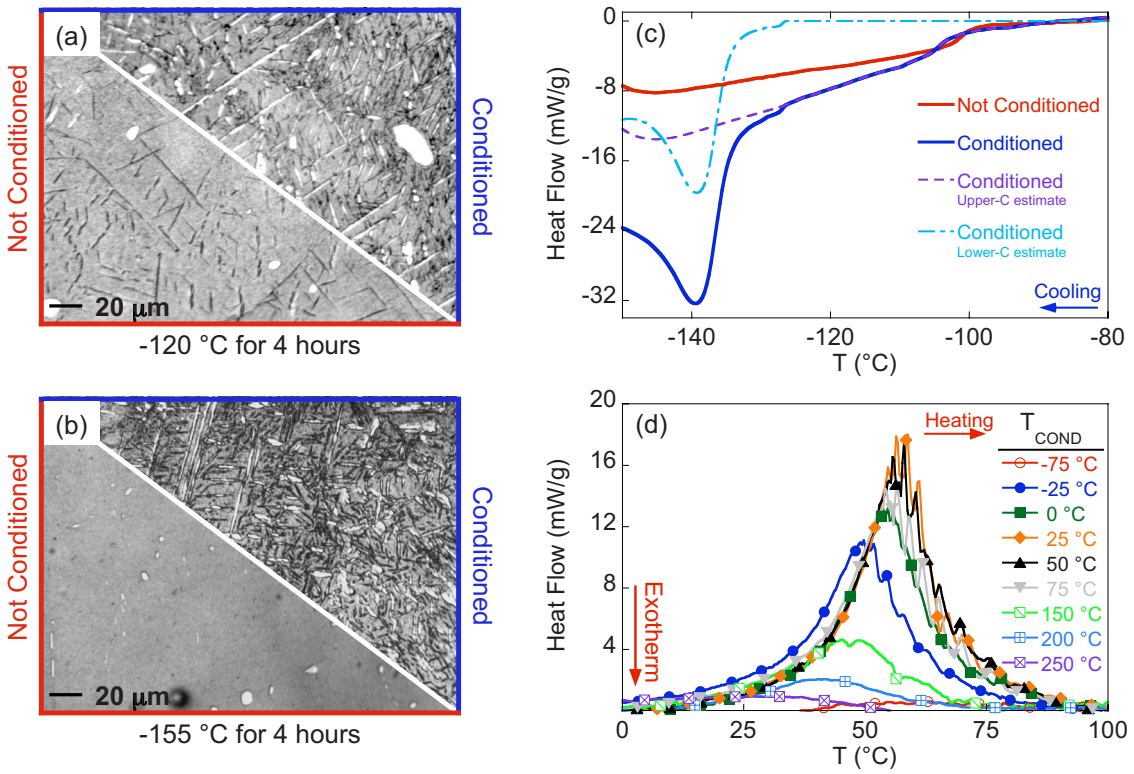

FIG. 2. (Color online) Optical micrographs after a 4 h isothermal hold at (a) −120 °C and (b) −155 °C with (upper-right triangle) and without (lower-left triangle) a previous 8 h conditioning treatment at room temperature. The high aspect ratio features are the α' product phase embedded in the surrounding δ matrix. Conditioning can be seen to increase the amount of transformation at both temperatures but it enables the transformation at −155 °C, suggesting that conditioning is responsible for the appearance of the lower C. (c) DSC traces (heat flow versus temperature) of the $\delta \rightarrow \alpha'$ transformation on cooling with and without conditioning. The upper and lower C components of the conditioned curve are estimated from the curve without conditioning (see text). (d) DSC traces showing the $\alpha' \rightarrow \delta$ reversion for various 8 h isothermal conditioning treatments at T_{COND}. An unconditioned specimen would exhibit results identical to the −75 and 250 °C traces.

ditioning actually enables transformation in the lower C, and that, without conditioning, only the mechanism responsible for the upper C is involved in the $\delta \rightarrow \alpha'$ transformation.[29]

DSC measurements corroborate the conditioning dependence illuminated in Figs. 2(a) and 2(b). Figure 2(c) shows DSC traces of the $\delta \rightarrow \alpha'$ transformation as a function of cooling. When the sample is not conditioned, a single, broad feature is observed in the DSC trace. With conditioning, however, a DSC trace reveals a new peak at lower temperature. Because optical metallography indicates that *only* the upper C exists without conditioning, then the unconditioned DSC trace can be assumed to be a result of transformation in the upper C and then scaled by a constant to estimate the contribution of the upper C with conditioning. This scaling is consistent with the increase in transformation with conditioning observed in Fig. 2(a). The difference between the raw DSC data with conditioning and the estimate for the conditioning-induced contribution to the DSC trace from the upper C provides an estimate for the contribution from the lower C. The new, conditioning-induced peak in the DSC appears to affect the amount of transformation only below −130 °C.

These results indicate that conditioning has a very profound effect on the kinetics of the $\delta \rightarrow \alpha'$ transformation but the results do not provide detailed insight into the mechanism of the conditioning effect. Thus, additional DSC measurements were undertaken to determine the temperature dependence of conditioning to illuminate the nature of the conditioning effect. Figure 2(d) shows DSC traces of the $\alpha' \rightarrow \delta$ reversion for 8 h isothermal holds at various conditioning temperatures T_{COND}. The areas under the reversion peaks in Fig. 2(d) are proportional to the volumetric amount of α' product phase formed during the transformation. Figure 2(d) reveals that the conditioning effect in Pu-1.9 at. % Ga has a significant temperature dependence. The maximum reversion peak area occurs between 25 and 50 °C but temperatures of −75 and 250 °C produce very little, if any, transformation-promoting effects. Any description of the conditioning effect must explain the increase in the amount $\delta \rightarrow \alpha'$ transformation observed in the micrographs and the DSC traces but that description must also encompass the temperature dependence of conditioning embodied in Fig. 2(d).

IV. CONDITIONING AS THE DEVELOPMENT OF NASCENT EQUILIBRIUM NUCLEI

The complexities of the Pu-Ga phase diagram [Fig. 1(a)] are driven by the presence of nearly degenerate phases. Hypothetical, schematic free energies as a function of Ga content for the δ, β, and α phases are shown in Fig. 3. At 210 °C [Fig. 3(a)], the β phase free energy for pure Pu is

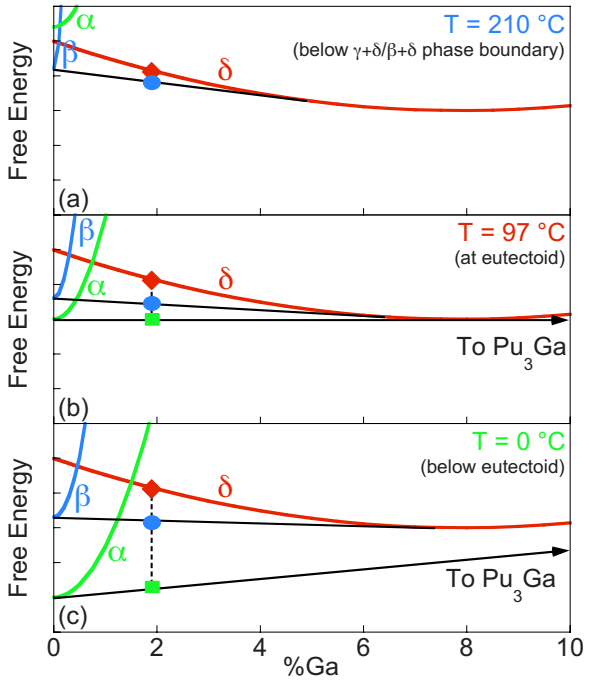

FIG. 3. (Color online) Schematic free-energy composition diagrams at various temperatures for the δ, β, and α phases of Pu-Ga. The decomposition, defined from the black tie lines, of the δ phase of the Pu-1.9 at. % Ga used in this study (red diamond) can lower the free energy of the system; these lower free energies are represented in (a), (b), and (c) by the blue circles, which correspond to the reduction in free energy in creating the β phase, and green squares, which correspond to the reduction in free energy in creating the α phase.

below that of δ, and it is then energetically favorable for the metastable δ phase of the alloy to transform into $\beta+\delta$. The free energy gained from this transformation is represented by the blue circle residing on the tie line connecting pure β-Pu with the Ga-containing δ phase. Reducing the temperature, as in (b), lowers the free energy for $\delta \rightarrow \beta+\delta$, but also permits the $\delta \rightarrow \alpha+\delta$ transformation, which results in a larger free-energy reduction represented by the green square. Reducing the temperature still further, as in (c), results in the eutectoid decomposition path, $\delta \rightarrow \alpha+Pu_3Ga$, with an even greater reduction in free energy.

While there is a chemical driving force for phase transformations into mixed phase microstructures, these transformations are not observed due to extremely slow Ga diffusion, stresses, or strains.[3–5,17] However, for a Pu-1.9 at. % Ga alloy, nuclei of the pure plutonium phases could form within the metastable δ phase via local distortions of the Pu lattice without diffusion of Ga.[32,33] The formation of Pu_3Ga nuclei is unlikely, as it would require significant Ga diffusion for a lean 1.9 at. % Ga alloy. Therefore, maintaining a sample of Pu-1.9 at. % Ga at a temperature within one of the mixed phase regions for an extended time could promote the formation of small, equilibrium-phase nuclei of order nanometers in radius.[34] These equilibrium nuclei are referred to as nascent because they would serve as the roots of a complete transformation given enough time (potentially thousands of years) for their evolution.

Once these postulated nascent equilibrium nuclei (NEN) form, they would be stable with respect to low-temperature excursions. As such, the presence of NEN would potentially have two transformation-promoting consequences for the $\delta \rightarrow \alpha'$ transformation: (1) increasing the number of available nucleation sites for the α' phase and (2) serving as progenitor nuclei for the growth of the α' phase.

In the first scenario and similar to grain boundaries or dislocations, NEN represent local deviations from the δ phase symmetry that could act as nucleation sites for the α' phase. In order to elicit the $\delta \rightarrow \alpha'$ transformation, these sites would likely need additional nucleation at low temperatures to overcome the symmetry and critical size differences between the β-like NEN, α-like NEN, and the critical nuclei that would grow into α' particles. By effectively increasing the number of available nucleation sites for the $\delta \rightarrow \alpha'$ transformation, the development of NEN would increase the amount of transformation through the formation of more α' particles or a reduction in the activation barrier necessary to nucleate the α' phase. This increased amount of transformation product is observed at −120 °C, where the amount of transformation yielded through conditioning is enhanced over that of an unconditioned sample [Figs. 2(a) and 2(c)].

In the second scenario, the NEN developed above the transformation temperature serve as progenitor nuclei for the growth of the α' phase at low temperature, where there is insufficient thermal activation for nucleation. As the size of an α' critical nucleus decreases with increasing undercooling, low-temperature nucleation could be effectively bypassed when the NEN average size and critical α' nucleus size are comparable, thus permitting growth directly from the NEN. This scenario is reflected in the data at −155 °C [Figs. 2(b) and 2(c)], where transformation at a low temperature is enabled by conditioning.

While the development of NEN provides a qualitative description for the observed behavior in the optical metallography and DSC studies of the $\delta \rightarrow \alpha'$ transformation with and without conditioning, the presence of these nuclei should be manifested in the behavior of the conditioning effect. Evidence for the existence of these NEN can be inferred through the temperature dependence of the conditioning effect and through the suppression of the conditioning effect with high-temperature treatments, where the NEN should be unstable due to increased atomic migration encouraging the dissolution of the nuclei into the higher-temperature equilibrium phases. Because the effects of conditioning occur in a matter of hours—saturating after about 8 h—we focus here on the formation and decay of α- and β-phase nuclei, and ignore the formation of Pu_3Ga as well as the γ phase, which likely has only a small driving force for formation from the δ phase in a Pu-1.9 at. % Ga alloy.

A. Temperature-dependent conditioning and classical nucleation

The temperature dependence of the formation of NEN is governed by classical heterogeneous nucleation, which can be described by

$$\dot{\mathcal{N}} = (\omega_0 e^{-\Delta G_M/RT})(n_0 e^{-\Delta G_c/RT}), \quad (1)$$

where $\dot{\mathcal{N}}$ is the rate of nucleation, ω_0 is a phonon frequency, ΔG_M is an activation barrier for thermal motion, n_0 is the

total number of nucleation sites in the sample, ΔG_c is the free energy required to create a nucleus, R is the gas constant, and T is the temperature.[36–38] In Eq. (1), the first term describes the rate at which atoms migrate in and out of a developing nucleus while the second term describes the energy to create a nucleus where ΔG_c includes the driving and inhibiting forces for heterogeneous nucleation

$$\Delta G_c = \frac{16\pi}{3}\frac{\tilde{S}\gamma^3}{(\Delta G_V + \Delta G_S)^2}, \tag{2}$$

where γ, ΔG_V, and ΔG_S are the surface energy, volume free energy, and strain energy, respectively, associated with the phase transformation, while $\tilde{S}$ is a shape factor for heterogeneous nucleation. The temperature dependence for ΔG_V can be estimated as

$$\Delta G_V = (T_0 - T)\Delta S, \tag{3}$$

where T_0 is the temperature at which the free energies of the two phases in question are equal and $\Delta S = \Delta H / T_0$ is the entropy of formation (with ΔH as the heat of transformation). Note that ΔG_V, the driving force, is defined as positive for temperatures below T_0.

If we let $A \equiv 16\pi\tilde{S}\gamma^3/3\Delta S^2$ and $B \equiv \Delta G_S/\Delta S$, then Eq. (1) becomes

$$\frac{\dot{\mathcal{N}}}{\omega_0 n_0} = \exp\left\{\frac{-1}{RT}\left[\Delta G_M + \frac{A}{(T_0 - T + B)^2}\right]\right\}, \tag{4}$$

where the temperature dependence of nucleation as a function of three parameters A, B, and ΔG_M is encompassed in the right side of the above equation. The left side of Eq. (4) describes the temperature-independent magnitude of the nucleation rate.

The areas under the curves of the DSC data from Fig. 2(d) are obtained by numerical integration and correspond to the measured heat of transformation which is proportional to the volumetric amount of transformation that occurs on cooling. Because the heat of transformation for the $\alpha' \rightarrow \delta$ reversion is not precisely known, the amount of transformation cannot be accurately correlated with optical metallography results. Thus, the amount of transformation as a function of conditioning temperature has been normalized to its maximum value, presented in Fig. 4 as red circles. The error bars are derived from instrumental noise.

The normalized experimental data of Fig. 4 are fit with two cases of Eq. (4): one case each for the nucleation of the α and β phases. The values of T_0 (i.e., the temperatures where $\Delta G^{\delta} = \Delta G^{\beta}$ and $\Delta G^{\delta} = \Delta G^{\alpha}$) are taken from Turchi *et al.*[39] while the value of $\Delta G_M = 12$ kJ/mol is determined as the best-fit value for both α and β nucleation. The maximum temperatures (T_{max}) for the nucleation of the α and β phases were fairly easily identified from the DSC data. By setting the derivative of Eq. (4) to zero at T_{max}, the fits of Eq. (4) to the data were reduced to a function of two free parameters: ΔG_M and A. The value of B was then calculated by solving a cubic equation that was a function of the experimentally observed T_{max} as well as the fit parameters ΔG_M and A. The values of A, in units of J-K^2/mol, and B, in units of K, determined from the fits are given in Fig. 4 for both nucleation processes. The temperature dependence of the nucleation of the α phase is represented by a green line while that of the β phase is represented by a blue line. The sum of the two nucleation processes is represented by a dark gray line, which overlaps the data points well.

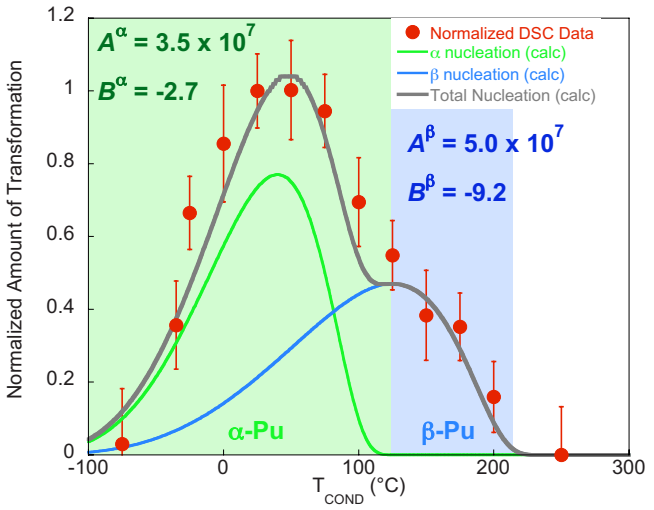

FIG. 4. (Color online) Evidence for the formation of NEN. The normalized amount of transformation as a function of T_{COND} (red circles) is determined by integrating the traces of Fig. 2(d). The green and blue shaded regions represent, respectively, the temperature ranges where the α and β phases are thermodynamically stable. The solid lines are fits to a classical nucleation equation describing nucleation of the equilibrium α (green line) and β (blue line) phases and their sum (dark gray line).

Deviations from the experimental data are evident on the low-T sides of the individual α and β nucleation curves. These deviations are likely a consequence of Eq. (3), which assumes a linear temperature dependence for ΔG_V. This linear temperature dependence is probably valid near T_0; but, at temperatures significantly below T_0, ΔG_V may deviate from the above assumption, resulting in discrepancy with the DSC data. It should be noted that the effects of self-irradiation on nucleation are not well understood, and no component of self-irradiation (e.g., radiation-enhanced diffusion) has been included in the description of the DSC data. The fits nonetheless provide compelling evidence, through the temperature dependence of the conditioning effect, that conditioning in Pu-1.9 at. % Ga is a result of the nucleation of equilibrium phases.

B. The decay of nascent equilibrium nuclei

In addition to the temperature dependence of nucleation, evidence for the development of NEN through conditioning is observed through the destruction of the positive effects of conditioning with high-temperature treatments. NEN, once formed, should be stable with respect to low-temperature excursions but they should dissolve back into the parent phase when subjected to high temperatures. An annealed and room-temperature-conditioned Pu-Ga sample was subjected to three post-conditioning treatments (i.e., isothermal holds for

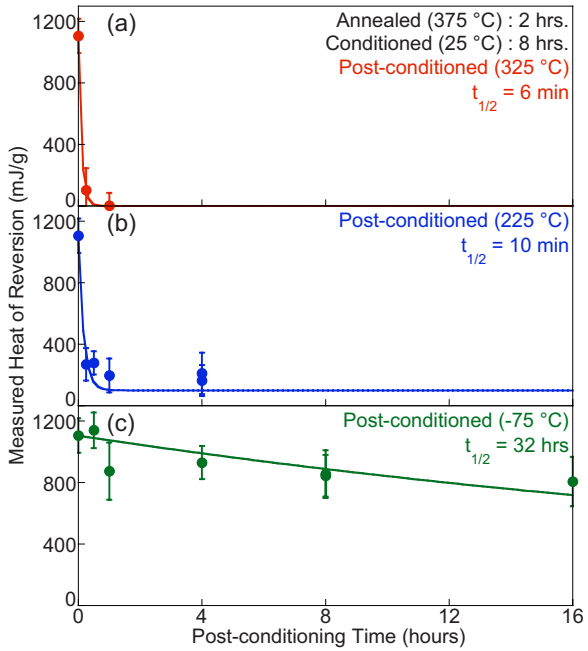

FIG. 5. (Color online) The decay of α-like NEN as a function of time at three key temperatures: (a) 325 °C, above the temperature range where conditioning occurs; (b) 225 °C, where small effects of conditioning attributed to β nuclei should occur; and (c) −75 °C, where only small amounts of α nuclei are expected to form. Solid lines are fits to a simple exponential decay equation used to extract the half life, $t_{1/2}$, for each post-conditioning temperature.

varying times immediately following the conditioning treatment) to investigate the destruction of the conditioning effect.

Figure 5 shows the results of post-conditioning treatments at three key temperatures: (a) 325 °C, within the stable δ phase field and where no second-phase nuclei are expected; (b) 225 °C, within the $\beta+\delta$ phase field, where β nuclei can form; and (c) −75 °C, within the $\alpha+Pu_3Ga$ phase field. In order to quantify the destruction of conditioning as a function of these post-conditioning treatments, the data have been fit with simple exponential decay equations of the form $\Delta H_R(t)=\Delta H_R(0)\exp(-t/t_{1/2})$, where $\Delta H_R(0)$ is the heat of reversion for zero post-conditioning (i.e., an optimally conditioned sample), t is the post-conditioning time, and $t_{1/2}$ is the NEN "half life," shown in Fig. 5. Post-conditioning at 325 °C shows a rapid suppression of the measured heat of reversion, with $t_{1/2}=6$ min. Similarly, post-conditioning at 225 °C shows a rapid decrease in the measured heat with $t_{1/2}=10$ minutes. However, unlike post-conditioning in the δ phase field, post conditioning in the $\beta+\delta$ phase field still permits a small amount of nucleation of the β phase, accounting for the observed measured heat of reversion near 100 mJ/g that persists for longer holds. Finally, post-conditioning at −75 °C yields, at most, a very slow decay of the measured heat of reversion ($t_{1/2}=32$ h). While the α-like NEN formed near room temperature should be stable at subambient temperatures, damage cascades from the alpha decay of Pu would likely contribute to the destruction of the nuclei. If a radiation damage cascade disrupts a NEN then that nucleus cannot easily reform at low temperature. The decay of the measured heat with different post-conditioning temperatures behaves as expected for a conditioning treatment described by the formation of NEN.

V. SUMMARY

From the results of our combined metallography and calorimetry study, we conclude that the conditioning effect in Pu-Ga is consistent with the development of NEN. Furthermore, we propose that the development of these nuclei is a route to affecting a martensitic transformation. In the case of Pu-1.9 at. % Ga, these NEN appear to be responsible for the double-C kinetics observed in the $\delta\rightarrow\alpha'$ transformation with the nuclei serving as additional nucleation sites in the upper C while serving as progenitor nuclei for transformation in the lower C. This mechanism ultimately arises due to a delicate balance between diffusion-limited decomposition, which permits the retention of a metastable phase, and the close proximity of the metastable and energetically preferred equilibrium phases within the free-energy landscape. The Pu-Ga system is a prime example of these two criteria but there is no strict rule within the above formalism that would exclude other systems from exhibiting a similar conditioning effect with dramatic implications for a displacive phase transformation.

ACKNOWLEDGMENTS

Lawrence Livermore National Laboratory is operated by Lawrence Livermore National Security, LLC, for the U.S. Department of Energy, National Nuclear Security Administration under Contract No. DE-AC52-07NA27344. This work was performed under LDRD.

[1] F. H. Ellinger, C. C. Land, and V. O. Struebing, J. Nucl. Mater. **12**, 226 (1964).
[2] N. T. Chebotarev, E. S. Smotriskaya, M. A. Andrianov, and O. E. Kostyuk, in *Plutonium 1975 and Other Actinides*, edited by H. Blank and R. Lindner (North-Holland, Amsterdam, 1976), p. 37.
[3] S. S. Hecker, Los Alamos Sci. **26**, 290 (2000).
[4] S. S. Hecker and L. F. Timofeeva, Los Alamos Sci. **26**, 244 (2000).
[5] L. F. Timofeeva, in *Aging Studies and Lifetime Extension of Materials*, edited by L. G. Mallinson (Kluwer Academic/Plenum, New York, 2001), p. 191.
[6] S. Y. Savrasov, G. Kotliar, and E. Abrahams, Nature (London) **410**, 793 (2001).
[7] G. Kotliar, S. Y. Savrasov, K. Haule, V. S. Oudovenko, O. Parcollet, and C. A. Marianetti, Rev. Mod. Phys. **78**, 865 (2006).
[8] A. Shick, J. Kolorenč, L. Havela, V. Drchal, and T. Gouder,

Europhys. Lett. **77**, 17003 (2007).
[9] J. H. Shim, K. Haule, and G. Kotliar, Nature (London) **446**, 513 (2007).
[10] C. A. Marianetti, K. Haule, G. Kotliar, and M. J. Fluss, Phys. Rev. Lett. **101**, 056403 (2008).
[11] K. T. Moore and G. van der Laan, Rev. Mod. Phys. **81**, 235 (2009).
[12] J. C. Lashley, J. Singleton, A. Migliori, J. B. Betts, R. A. Fisher, J. L. Smith, and R. J. McQueeney, Phys. Rev. Lett. **91**, 205901 (2003).
[13] S. K. McCall, M. J. Fluss, B. W. Chung, M. W. McElfresh, D. D. Jackson, and G. F. Chapline, Proc. Natl. Acad. Sci. U.S.A. **103**, 17179 (2006).
[14] M. E. Manley, A. H. Said, M. J. Fluss, M. Wall, J. C. Lashley, A. Alatas, K. T. Moore, and Yu Shvyd'ko, Phys. Rev. B **79**, 052301 (2009).
[15] L. F. Timofeeva, Metal Sci. Heat Treat. **46**, 490 (2004).
[16] T. B. Massalski and A. J. Schwartz, J. Alloys Compd. **444-445**, 98 (2007).
[17] P. E. A. Turchi, L. Kaufman, S. Zhou, and Z.-K. Liu, J. Alloys Compd. **444-445**, 28 (2007).
[18] W. G. Wolfer, Los Alamos Sci. **26**, 274 (2000).
[19] A. J. Schwartz, M. A. Wall, T. G. Zocco, and W. G. Wolfer, Philos. Mag. **85**, 479 (2005).
[20] A. Kubota, W. G. Wolfer, S. M. Valone, and M. I. Baskes, J. Comput. Aided Mater. Des. **14**, 367 (2007).
[21] S. S. Hecker, Metall. Mater. Trans. A **39A**, 1585 (2008).
[22] S. S. Hecker, D. R. Harbur, and T. G. Zocco, Prog. Mater. Sci. **49**, 429 (2004).
[23] A. J. Schwartz, H. Cynn, K. J. M. Blobaum, M. A. Wall, K. T. Moore, W. J. Evans, D. L. Farber, J. R. Jeffries, and T. B. Massalski, Prog. Mater. Sci. **54**, 909 (2009).
[24] J. T. Orme, M. E. Faiers, and B. J. Ward, in *Plutonium 1975 and Other Actinides*, edited by H. Blank and R. Lindner (North Holland, Amsterdam, 1976), p. 761.
[25] B. Oudot, K. J. M. Blobaum, M. A. Wall, and A. J. Schwartz, J. Alloys Compd. **444–445**, 230 (2007).
[26] Y. Imai, M. Izumiyama, and K. Sasaki, Sci. Rep. Res. Inst. Tohoku Univ. A **18**, 39 (1966).
[27] J. J. Rechtien and R. D. Nelson, Metall. Trans. A **4**, 2755 (1973).
[28] K. J. M. Blobaum, C. R. Krenn, M. A. Wall, T. B. Massalski, and A. J. Schwartz, Acta Mater. **54**, 4001 (2006).
[29] J. R. Jeffries, K. J. M. Blobaum, M. A. Wall, and A. J. Schwartz, Acta Mater. **57**, 1831 (2009).
[30] K. T. Moore, M. A. Wall, and A. J. Schwartz, J. Nucl. Mater. **306**, 213 (2002).
[31] J. R. Jeffries, K. J. M. Blobaum, M. A. Wall, and A. J. Schwartz, J. Nucl. Mater. **384**, 222 (2009).
[32] J. W. Cahn and J. E. Hilliard, J. Chem. Phys. **31**, 688 (1959).
[33] J. W. Cahn, Acta Metall. **9**, 795 (1961).
[34] The critical radii of the NEN are given by $r_c=2\sigma/g_v$, with σ as the surface energy in J/cm^2 and g_v as the volume free energy in J/cm^3. Using $\sigma \sim 100\times10^{-7}$ J/cm^2 and $g_v \sim 100$ J/cm^3 at 25 °C (Refs. 28 and 35), $r_c \sim 1$ nm for α-like nuclei near room temperature.
[35] P. H. Adler and G. B. Olson, Metall. Trans. A **19A**, 2705 (1988).
[36] R. Becker and W. Döring, Ann. Phys. **24**, 719 (1935).
[37] K. Binder, Phys. Rev. A **29**, 341 (1984).
[38] D. W. Oxtoby, J. Phys.: Condens. Matter **4**, 7627 (1992).
[39] P. E. A. Turchi, L. Kaufman, Z. -K. Liu, and S. Zhou, LLNL Report No. UCRL-TR-206658, 2004 (unpublished).